Catalytic mechanism and protein engineering of copper-containing nitrite reductase

Wijma, Hein Jakob

Citation
Wijma, H. J. (2006, February 9). *Catalytic mechanism and protein engineering of copper-containing nitrite reductase*. Retrieved from https://hdl.handle.net/1887/4302

Version:	Corrected Publisher's Version
License:	Licence agreement concerning inclusion of doctoral thesis in the Institutional Repository of the University of Leiden
Downloaded from:	https://hdl.handle.net/1887/4302

Note: To cite this publication please use the final published version (if applicable).

Chapter 2

Copper-containing Nitrite Reductase

2.1 General

Copper-containing nitrite reductase (NiR) is an enzyme from the denitrification pathway (scheme 1).

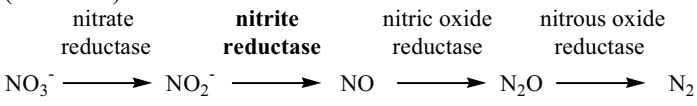

(1)

Denitrification globally recycles (*56*) fixed nitrogen (NO_3^-, NO_2^-) to the atmosphere (N_2) while NO and N_2O may escape as by-products, which act as ozon scavengers and greenhouse gases (*57, 58*). Cu-containing nitrite reductases are found in all three kingdoms of life; in eubacteria (*56*), archaea (*59, 60*), and amongst eukaryotes in denitrifying fungi (*61*). As for pathogens, NiR is known to enhance the resistance against human sera in *Neisseria gonorrhoeae* (*62*) and allows both *N. gonorrhoeae* and *N. meningitidis* to respire on nitrite under the microaerobic conditions encountered during host colonization and disease (*63, 64*). Furthermore, there is an interest in applying NiR in amperometric biosensors to selectively monitor nitrite in natural waters and waste streams (*65-67*).

Besides the copper-containing nitrite reductases there also exist iron-containing nitrite reductases (mostly referred to as cd_1 nitrite reductases). Both types of enzyme catalyse the dissimilatory reduction of nitrite ($NO_2^- + 2H^+ + e^- \rightarrow NO + H_2O$) during denitrification and both were recently assigned EC 1.7.2.1 (previously 1.7.99.3 for NiR, 1.9.3.2 for iron-containing nitrite reductase). *In vivo*, these dissimilatory nitrite reductases can replace each other (*68*). In eubacteria, copper-containing nitrite reductases occur in a larger variety of organisms with more different habitats than the iron-containing nitrite reductases (*69*). There also exist assimilatory nitrite reductases, which catalyse the reduction of nitrite to ammonia (*70*).

For copper-containing nitrite reductase it is shown in chapter 3 that it can also catalyse the reverse reaction ($NO + H_2O \rightarrow NO_2^- + 2H^+ + e^-$). Other reactions catalysed by NiR are the production of nitrous oxide from nitrite and nitric oxide ($NO + NO_2^- + 4H^+ + 3e^- \rightarrow N_2O + 2H_2O$ (*71*)), and from nitrite and hydroxylamine ($NH_2OH + NO_2^- + H^+ \rightarrow N_2O + 2H_2O$ (*72-74*). Furthermore, super oxide dismutase activity ($2O_2^{\bullet-} + 2H^+ \rightarrow O_2 + H_2O_2$) and the reduction of oxygen to hydrogen peroxide ($O_2 + 2H^+ + 2e^- \rightarrow H_2O_2$) are known for NiR (*75, 76*).

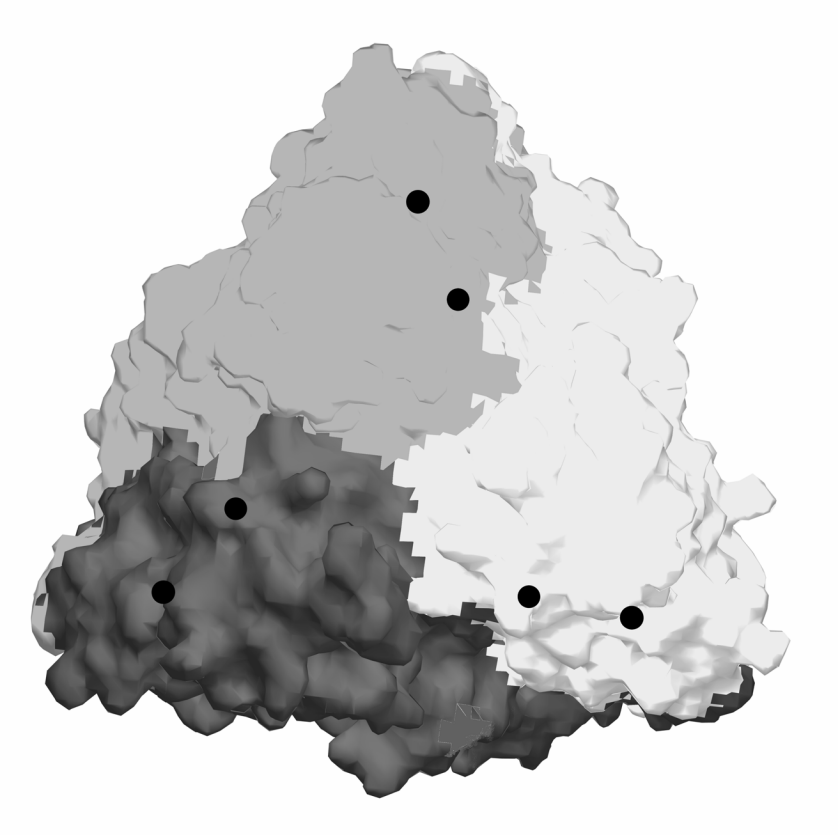

Figure 1: Trimeric structure of copper-containing nitrite reductase
The surface of the different monomers is indicated with different shades of grey. The positions of type-1 and type-2 sites (located inside the NiR) are indicated by black dots. The type-2 sites are situated near the interfaces.

2.2 Structure, type-2 site and related active sites

NiR is a homotrimer in which every monomer contains on type-1 electron relay site and one type-2 catalytic site (*77*). The monomers are packed closely together (Figure 1) and each monomer consists of two cupredoxin domains (see section 1.3). The type-1 site accepts electrons from the physiological electron donor (*78-80*) and transfers them to the catalytic type-2 site (*81*).

In the type-2 site of NiR, the Cu is bound by three histidines while at the fourth position nitrite can bind (Figure 2), replacing water or hydroxyl. In the EPR spectrum of the enzyme (Figure 3) the type-2 site has a larger hyperfine splitting than the type-1 site, which can be used to monitor the titration of nitrite (*82*). The optical spectrum of the type-2 site is very weak compared to that of the type-1 site, and for the first time described in this thesis (Figure 1A in chapter 6). An aspartate, a histidine and a bridging water molecule are involved (*83-87*) in the binding of nitrite and in catalysis (see Figure 2; also section 2.6).

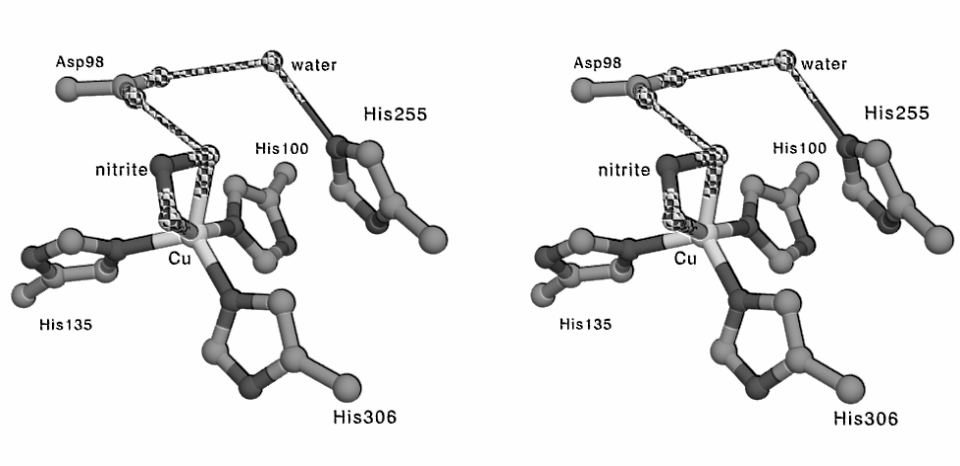

Figure 2: Detail of the catalytic type-2 site of NiR
The representation is based on the structure of *Alcaligenes faecalis* S-6 NiR complexed with nitrite (*3*) 1SJM. Different atoms are represented by different shades of gray or by a chess-board pattern (for oxygen). Normal bonds are shown by cylinders and hydrogen bonds are shown by thin connections.

Apart from the type-2 site as encountered in NiR, other copper-containing enzymatically active sites occur in nature. The closest relative to the type-2 active site of nitrite reductase is the trinuclear site of blue oxidases (*19*). The trinuclear active site of blue oxidases is also classified as type-2,3 or type-4, and catalyses the reduction of oxygen (O_2 + $4H^+$ + $4e^-$ $\rightarrow 2H_2O$). Furthermore, some other copper enzymes have been classified as containing a type-2 site based upon the similar EPR spectrum of their active sites. These include nitrosocyanin (see section 1.3) and unrelated enzymes, such as amine oxidases (catalyses $RCH_2NH_3 + O_2 \rightarrow RCHO + NH_3 + H_2O_2$), galactose oxidase ($RCH_2OH + O_2 \rightarrow RCHO + H_2O_2$), and Cu-Zn superoxide dismutase (*88-92*). Further, dinuclear copper-sites, all classified as type-3, exist that can have various functions such as oxygen transport (*93*) and phenoloxidase activity (*94*). A tetranuclear copper site (Cu_Z) exists (*95*) in nitrous oxide reductase, which catalyses the reaction $N_2O + 2H^+ + 2e^- \rightarrow N_2 + H_2O$. In cytochrome c oxidase, a mononuclear Cu_B and a heme a_3 are combined into a binuclear centre that catalyses the four-electron reduction of oxygen to H_2O (*96*). Thus, in many enzymes copper is involved in facilitating redox reactions.

2.3 Diversity of NiR

Based on sequence-alignment and structural differences, copper-containing nitrite reductases can be grouped in class I and class II (*97*). In Figure 3 the best characterized members of the different classes are shown in a clustal W based tree. The differences between class I and II are much larger than between the members of class I, and PCR primers useful to pick up any class I NiR will not detect class II NiRs (*98*). The dependence of catalytic activity on pH of all characterized class I NiRs is identical, while the only class II NiR characterized up to now differs in its pH dependence (*vide infra* section 2.7). Within class I, Yoshie (*98*) found in a larger set of NiR sequences that there exist three subclasses, coinciding with subclass IA, IB, and IC in Figure 3. These subclasses seem to agree with the physiological electron donors, i.e., for class IA pseudoazurin, for class IB cyt c_{551}, for class IC cyt c_2 (see section 2.4).

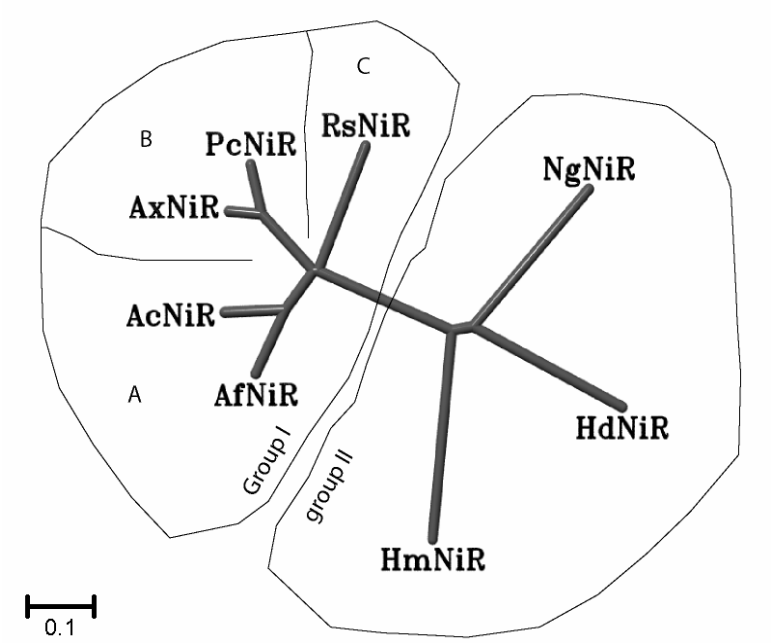

Figure 3: Different classes and subclasses of copper-containing nitrite reductases
Distance scale is shown as a bar. The classes and subclasses are indicated in the figure. NgNiR from *Neisseria gonorrhoeae*; HdNiR from *Hyphomicrobium_denitrificans*; HmNiR from *Haloarcula marismortui*; AfNiR from *Alcaligenes faecalis* S-6; AcNiR from *Achromobacter cycloclastes*; AxNiR from *Alcaligenes xylosoxydans xylosoxydans*, PcNiR from *Pseudomonas chlororaphis*; RsNiR from *Rhodobacter sphaeroides.*

It is common in the literature to classify NiRs as either blue or green based on their spectroscopic properties. The blue NiRs (mainly class IB) have an extinction ratio of the 460 and 600 nm bands of approximately 0.2 and an axial EPR spectrum while the green NiRs (class IA and IC) have an A_{460}/A_{600} ratio of approximately 1 and a rhombic EPR spectrum. However, as pointed out by Suzuki (*99*), many other NiRs (mainly class II) have spectroscopic properties that are either intermediate or different. We notice that the dihedral angle θ[1], which largely determines the spectroscopic properties of type-1 sites (see chapter 6 and 7 for more details), of all NiRs are in a region where small changes drastically affect the type-1 site spectroscopic properties (Figure 1 and 7 in chapter 6). Thus, the clear spectroscopic differences between green and blue NiRs may reflect only small differences in their type-1 sites. In our view, spectroscopic properties are unsuitable as a primary criterion for classification of NiRs.

[1] θ is the angle between the planes through N-Cu-N and S-Cu-S in the type-1 site

2.4 Electron donors and their relation to catalytic activity

The physiological electron donor for *Achromobacter cycloclastes* and *Alcaligenes faecalis* NiR (class IA) is pseudoazurin. The proof for this is formed by the specific complexes formed during electron transfer (*79, 80, 100*), the catalytic turnover rate which is as high as with the best synthetic electron donors (Table 1), and the relatively high second order rates of reduction of NiR by pseudoazurin (3.3×10^5 M^{-1} s^{-1} for *A. faecalis* (*67*) and 7.4×10^5 for *A. cycloclastes* (*101, 102*)). For NiR from *Alcaligenes xylosoxidans* (class IB) an early investigation reported that cyt c_{552} was the electron donor to NiR (*74*) and recently a high (4.0×10^5 M^{-1} s^{-1}) second order rate of *Alcaligenes xylosoxidans* NiR reduction by cyt c_{551} (*103*) was reported. For *Rhodobacter sphaeroides* NiR (Class IC), a cytochrome c_2 appears to be the physiological electron donor (*104*). As for the class II NiRs, a cyt c_{552} is suggested (*105*) to be the electron donor to the NiR of *Nitrosomonas europaea* and azurin is suggested (*97*) to be the electron donor to *Neisseria* NiR. In these two cases no proof is available for efficient electron transfer with the NiR. Thus, the most certain physiological electron donors are pseudoazurin for class IA NiRs and cyt $c_{551/552}$ for class IB.

It has been suggested that azurin is the electron donor for the class IB NiR from *A. xylosoxidans* (*106*). This is in contrast to an earlier investigation that examined cyt c_{552} and azurin from the same organism, and assigned cyt c_{552} instead of azurin as the electron donor for NiR (*74*). Significantly, the data in Table 1 show that the azurin for both members of class IB NiRs gives a 100-fold lower catalytic activity than a suitable synthetic electron donor, while in the case of pseudoazurin these catalytic activities are nearly the same. For cd_1 nitrite reductase, azurin was originally misidentified as the electron donor, but currently pseudoazurin and cyt c_{551} have been shown to be the *in vivo* electron donors (*107*). Azurin is more likely to be the electron donor for cyt c peroxidase as it enhances the resistance against hydrogen peroxide (*34*).

To obtain efficient protein-protein electron transfer, both the electrostatic interactions between the proteins and the shape of their surfaces need to match precisely (*108*). In Table 1 the catalytic activities of NiR with different electron donors are compared at pH 7 and pH 6 (class I NiRs have the same pH dependence). The low catalytic activities of the horse-heart cyt c, yeast cyt c, and azurins suggest that non-physiological protein-protein electron transfer is too inefficient to supply electrons at a rate that matches the rate of the catalytic site of the NiR. For artificial electron donors these conditions may be more easily met. The diffusion rates of small synthetic electron donors are expected to be faster than those of proteins, which may alleviate the need for favourable electrostatic interactions to bring the reactants together. Indeed, the catalytic activities with some synthetic electron donors are nearly identical to those with physiological electron donors.

Table 1: Catalytic activities of NiRs with different electron donors

pH	Class	Organism	Electron Donor	k_{cat} (s^{-1})	K_M NO_2^- (μM)	k_{cat}/K_M NO_2^- (10^6 M^{-1} s^{-1})	Reference
7	IA	*Alcaligenes faecalis S-6*	Pseudoazurin [A]	392	36	3.85	chapter 3
		"	MV-SDT [B]	338	74	4.57	chapter 6
		"	DPIP [C]	24	-	-	present study
		"	Azurin [D]	1.3	-	-	(*109*)
	IB	*Alcaligenes xylosoxidans*	Azurin [A]	14	-	-	(*110*)
		"	BV-SDT	470	23	20.4	(*86*)
		Pseudomonas chlororaphis	Azurin [A]	0.2	-	-	(*111*)
		"	MV-SDT	81	-	-	(*111*) [E]
	II	*Haloarcula marismortui*	BV-SDT	573	-	-	(*112*)
	II	*Neisseria gonorrhoeae*	MV-SDT	97	-	-	(*97*)
	?	*Fusarium oxysporum*	NADH-PMS	345	49	7.05	(*61*)
6	IA	*Achromobacter cycloclastes*	horse-heart cyt c	15	5.6	2.7	(*81, 113*)
		"	TMPD	23	-	-	(*114*)
		Alcaligenes faecalis S-6	horse-heart cyt c [F]	53	-	-	present study
		"	Pseudoazurin [A]	1478	49	30.1	chapter 3
	IB	*Alcaligenes xylosoxidans*	BV-SDT	1640	-	-	(*86*)
		"	TMPD	12	-	-	(*114*)
	IC	*Rhodobacter sphaeroides*	yeast cyt c	50	-	-	(*87*)
5.5	II	*Hyphomicrobium denitrificans*	BV-SDT	320	620	0.52	(*115*)

[A] from the same organism; [B] Earlier 387 s^{-1} (*80*) and 233 s^{-1} (*116*) were reported; [C] obtained in 50 mM MES-HEPES-NaOH pH 6.5 at 25 °C; [D] azurin from *Pseudomonas aeruginosa*; [E] rate of methyl viologen disappearance; [F] assays were done at 25 °C with 400 μM of reduced horse-heart cyt c in 50 mM MES-NaOH buffer pH 6.2 with 2 mM of nitrite, the K_M for the horse-heart cyt c was 48.1 ± 6.6 μM

Abbreviations: TMPD = N,N,N',N'- tetramethyl-p-phenylenediamine, MV-SDT = methyl viologen *in situ* reduced by sodium dithionite; BV-SDT, idem for butyl viologen; PMS-NADH, phenazine metasulfate reduced *in situ* by NADH, DPIP, 2,6-dichlorophenol indophenol

At the same time, the reduction potential of a synthetic donor may influence the rate of electron transfer, a low reduction potential speeding up the electron transfer rate. The latter effect agrees with the high rates (Table 1) obtained with strong electron donors (methyl viologen -446 mV versus NHE, benzyl viologen -352 mV, methylene blue 11 mV, PMS 92 mV) versus those obtained with TMPD (270 mV versus NHE) and DPIP (217 mV versus NHE). However, also the efficiency of synthetic electron donors appears to depend to a certain extent on electrostatics and surface properties, as in the case of *Fusarium oxysporum NiR,* for which methyl viologen gives a 90 % lower rate than PMS (*61*), although methyl viologen is a stronger electron donor. Thus, all class I NiRs have similar catalytic activity at a given pH, and the large span of catalytic activities reported for NiRs (Table 1) is mainly the result of variation in the efficiency of the electron donors.

The use of a slow electron donor may mask a change in the catalytic properties of the NiR, since it makes electron transfer to the type-1 site the rate-limiting step. Possible examples are the observation of 50% catalytic activity for type-2 Cu depleted NiR with TMPD as the electron donor (*114*) and the observation of 70% catalytic activity for a NiR mutant in which the catalytically essential His255 was removed by site-directed mutagenesis (*110*) when azurin was employed as the electron donor. When the inefficiency of the electron donor (Table 1) is taken into consideration, these activities are a few percent of the full catalytic activity, which is in agreement with the loss of an important part of the active site (*117*). Thus, to study the catalytic activity of NiR, the electron donor should be fast enough to monitor the true activity of the NiR rather than the rate of electron transfer to the NiR.

Various synthetic electron donors for NiR react with the produced nitric oxide, resulting in the formation of N_2O, N_2, NH_4 or mixtures of those (*56, 118*). The concentration of electron donor versus time is therefore not a good indicator of the enzyme activity and the nitrite concentration versus time should be used instead. With protein electron donors on the other hand, the disappearance of the reduced form of the donor is a reliable indicator for the enzyme activity. Physiological electron donors like pseudoazurin allow monitoring the true catalytic rate of the NiR spectroscopically, while they are not highly toxic nor highly sensitive to oxygen like some of synthetic electron donors in Table 1.

A disadvantage of most physiological electron donors is their limited availability (*76, 119*) (approximately 1 mg of physiological electron donor is needed for a single activity assay and yields of 1 mg per litre of culture are normal for purification from the original organism). For pseudoazurin, it was possible to improve the existing (*120*) over-expression system by lowering both the pre-incubation temperature and expression temperature (*121*), improving the yield 20-fold (chapter 3) to more than 500 mg per litre of culture. Also for the NiR of *Alcaligenes faecalis* S-6 (yields > 200 mg per litre of culture, chapter 6) and for the NiR from *Alcaligenes xylosoxidans* (*122*) dramatically higher yields could be obtained by pre-incubation and expression at lower temperatures.

In chapter 4, a novel electron donor for NiR is introduced, i.e. a rotating disk electrode. The rotation is necessary to prevent nitrite depletion near the electrode surface while measuring activity. The advantage of using this electrode is that the dependence of turnover rate on nitrite concentration and pH can be investigated much faster and more accurately than with a solution electron donor (*123*). In our case, a drawback of the rotating disk electrode was that absolute activities could not be determined since the amount of NiR immobilized on the electrode was too low to be measured. Thus, assays for the absolute catalytic activity (with pseudoazurin) and for the relative activity under different conditions (with a rotating disk electrode) are now available for the study of *Alcaligenes faecalis* NiR.

2.5 Effect of ionic strength on k_{cat}

Studies of the effect of ionic strength on catalytic activity in the presence of a physiological electron donor have not been reported elsewhere. The activities versus pH reported in chapter 3 and chapter 4 differ slightly from each other, depending on the buffer. This was briefly investigated further. At pH 6.5 and at 240 μM pseudoazurin, in a plot of catalytic activity versus ionic strength a bell-shaped curve is observed, the activity increasing from 450 s^{-1} (at an ionic strength of 20 mM) to 650 s^{-1} (at approximately 130 mM), and decreasing again at higher ionic strength (Figure 4). The bell-shaped curve is commonly observed in protein-protein electron transfer and normally indicates (*124*) that at low ionic strength the electron donor (pseudoazurin) may get locked in an unproductive complex with the electron acceptor (NiR), while at higher ionic strength the electrostatic interactions are weakened (*79, 80*). In the case of pseudoazurin it is also possible that at low ionic strength (part of) the pseudoazurin has dimerized, as was shown for *Paracoccus pantotrophus* pseudoazurin (*125*). In *Haloarcula marismortui* NiR the effect of ionic strength on catalytic activity in the presence of a synthetic strong electron donor was reported. This NiR is optimally active in 2 M NaCl (*112*), in agreement with its origin from a halophilic organism. The dependence on ionic strength shows that activity assays with a physiological electron donor should be done at the same ionic strength if the results are to be fully comparable to each other.

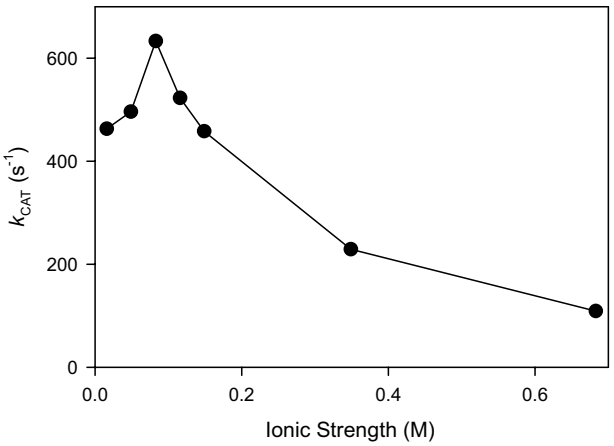

Figure 4: Ionic strength dependence of catalytic activity with physiological electron donor.
The activity was determined at pH 6.5 in 20 mM MES-NaOH buffer with nitrite (2 mM) at 25 °C. The ionic strength was varied by addition of NaCl. The concentration of pseudoazurin (reduced) was 240 μM, the concentration of NiR was 3 nM. For assay conditions see the materials and methods of chapter 3.

2.6 Catalytic Mechanism

One of the three important questions (*56*) for the catalytic mechanism of NiR is whether the nitrite binds to the oxidized or to the reduced type-2 site. It has been argued (*69, 126*) that the nitrite binds first to the reduced type-2 site because in inorganic model complexes for the type-2 site the copper is reduced before the nitrite binds (*127, 128*) and becauses the K_M for nitrite is at least 10-fold lower than the K_d of the oxidized type-2 site for nitrite (*82*). Others advocate binding to the oxidized type-2 site first (*86, 129*) since the pre-reduced NiR reacts slowly with nitrite (*54, 130*) and since the reduced type-2 site shows a low occupancy at the position of the fourth ligand (*54, 83, 131*). These observations suggest that the reduced type-2 site is tri-coordinate and binds nitrite with low affinity. From the result reported in chapter 4 it appears that during turn-over nitrite can both bind to the oxidized and to the reduced type-2 site (Figure 5), and that both pathways contribute significantly to the overall rate. The results from chapter 5 indicate that there is indeed a reduced inactive state (three-coordinate type-2 site) which is in slow equilibrium with the reduced active enzyme (four coordinate type-2 site). Thus, it appears that nitrite can bind to the reduced type-2 (lower route in Figure 5) as well as to the oxidized type-2 site (upper route in Figure 5).

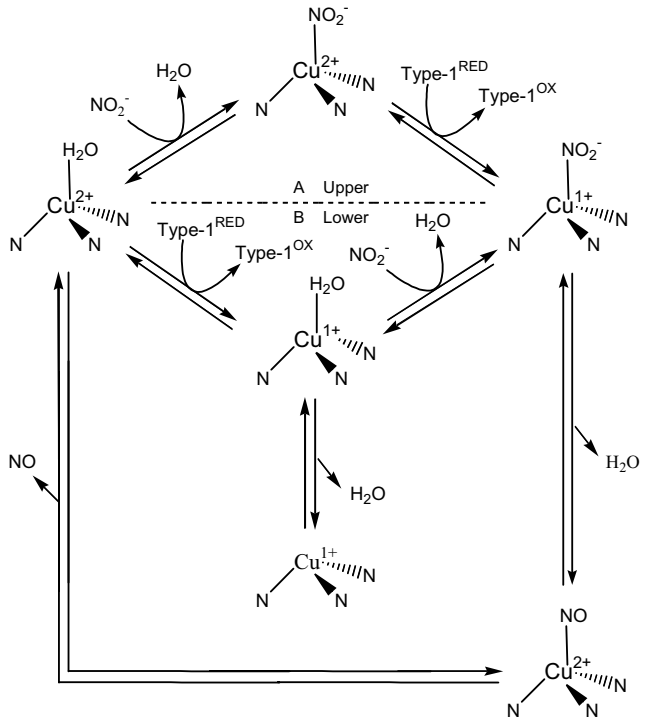

Figure 5: Catalytic Cycle of Copper-containing Nitrite Reductase
Type-1 refers to the type-1 copper site from which the type-2 site accepts an electron.

The two other questions are whether the nitrite binds to the Cu via its oxygen or via its nitrogen and whether the H_2O/OH^- or the NO leaves first during the reaction. The answer to the second question may depend on the redox state of the Cu atom (*69, 126*). Based on hard-soft acid-base (HSAB) theory (*132*), the Cu^{1+} may prefer ligation by nitrogen, while the Cu^{2+} may prefer the "harder" oxygen atoms. In model complexes this is indeed found (*126*). However, in crystal structures of substrate-bound oxidized NiR (*3*), the nitrite is bound with Cu-O distances of 2.1 and 2.3 Å, and a Cu-N distance of 2.3 Å (almost "face-on"; in face-on binding mode the distances from the Cu to the ligandatoms are equal). Nitric oxide is bound "side-on" to the copper atom with the ligands atoms equidistant from the Cu at 2.0 Å. It is suggested that upon reduction of the Cu, the bound nitrite rearranges, bringing the nitrogen closer to the Cu (in agreement with HSAB rules) and releasing one of the oxygen atoms as H_2O or OH^- (*3*). Thus, in NiR the nitrite binds almost face-on to the oxidized type-2 site, the bound nitrite possibly rearranges when the type-2 copper is reduced, followed by release of water, and in the copper-nitrosyl intermediate the nitric oxide is bound side-on.

The absolutely conserved active site residues Asp98 and His255 are important for catalysis, as shown by the 100-fold decrease in k_{cat} for D98A (*Achromobacter cycloclastes* numbering), D98E, and D98N and the 1000-fold decrease in k_{cat} for H255A, H255D, H255K, and H255R (*85-87*). The K_M values for nitrite increase 100-fold for the Asp98 mutations while K_M increases only 0.5 to 10-fold for the His255 mutations (*85-87, 133*). From crystal structures, and various spectroscopic investigations, it appears that there is a hydrogen bond between the nitrite and the Asp98 (*83, 84, 87, 131, 134*). The His255 is observed to form a hydrogen bond to Asp98 via a bridging water (see Figure 2) (*84, 85*). The observations are in agreement with a role for Asp98 in binding the nitrite and donating protons while the role of His255 is in donating protons to the Asp98 via the bridging H_2O (*84, 85, 129*) and possibly by ensuring the proper orientation of Asp98 (*86*).

2.7 Effect of Nitrite concentration and pH on Catalytic Activity

In chapter 4 it is shown for the first time that NiR does not display the normal Henri-Michaelis-Menten kind of kinetics but instead has two affinity constants (K_M^A and K_M^B) and two apparent velocities (k_{cat}^A and k_{cat}^B) according to equation 2,

$$k_t(S) = (k_{cat}^A[S] + k_{cat}^B[S]^2/K_M^B) / (K_M^A + [S] + [S]^2/K_M^B)\} \quad (2),$$

in which $k_t(S)$ is the rate of substrate conversion per subunit of NiR. The k_{cat}^A, k_{cat}^B, K_M^A, and K_M^B are complicated functions of the rate constants appearing in Figure 5. In a simplification, k_{cat}^A and K_M^A are the Michaelis constants of the lower route while k_{cat}^B and K_M^B correspond with the upper route (Figure 5). The k_{cat}^A and k_{cat}^B differ since the electron transfer rate from type-1 to type-2 site, which is rate-limiting for the NiR (*86, 115*), depends on the ligand that is bound to the type-2 site (nitrite for the upper route and for the lower route H_2O/OH^-, depending on pH, chapter 4). The K_M^A and K_M^B differ, since for K_M^A the binding is to the reduced copper atom and for K_M^B the binding is to the oxidized Cu atom, while, in addition, K_M^A is a more complicated function of the kinetics of the system than K_M^B (chapter 4). At infinitely high nitrite concentration, all catalysis will occur via the upper route. Since below pH 6.5, $K_M^A < K_M^B$ and $k_{cat}^B < k_{cat}^A$ there is a nitrite concentration where the catalytic activity is at its maximum ($\cong k_{cat}^A \times$ [NiR]) followed by a decrease to a plateau where the activity becomes constant ($= k_{cat}^B \times$ [NiR]). Between pH 6 and 8 and at low nitrite concentrations (< 10 mM), the deviations from normal Henri-Michaelis-Menten kinetics are small (Figure 5B in chapter 3) because only the lower route is relevant in this range.

All class I NiRs (*72, 82, 86, 87, 116*) display bell-shaped curves (Figure 1A in chapter 4) of their catalytic activity as a function of pH, with pKa values around 5 and 7, and a maximum around pH 6. In chapter 4, it is shown that this pH optimum depends on the nitrite concentration used in the assays, lower concentrations of nitrite lowering the pH optimum. This is in line with the random-sequential mechanism and is discussed in more detail in chapter 4. The only class II NiR characterized with respect to activity versus pH is from *Hyphomicrobium denitrificans*. It displays an ever increasing activity towards low pH down to at least pH 4.5. No deuterium isotope effect could be detected (*87*), which may either mean that proton transfer is truly not a rate-limiting step for the NiR or that the yeast cyt c, which was used as the electron donor, was rate-limiting.

The activity versus pH profiles of D98A, D98N, and H255A of various NiRs display similar bell-shaped curves (*86, 87*) as the wt. This suggests that neither His255 nor Asp98 are responsible for the changes in catalytic activity. A reaction that might be connected with the pKa around pH 7 is replacement of the Cu bound water by hydroxyl (*87, 135*), which is expected to lower the midpoint potential of the type-2 site. This is indeed observed (a shift of -100 mV is observed going from pH 6 to 8 for *Alcaligenes xylosoxidans* NiR (*136*)). This would slow down the rate-limiting electron transfer step, in agreement with observation (*136*). The reason why the rate of catalysis (and of electron transfer) goes down below pH 5 is currently unclear.

The driving force for the reaction is strongly influenced by the nitrite-nitric oxide equilibrium; this couple has a -118 mV per pH unit dependence on pH (chapter 3). The commonly cited value of E_0' (pH 7) of ≈ 0.35 V versus NHE (*56, 137*) for the NO_2^-/NO redox pair is correct but less useful, since the concentration of nitric oxide is expressed in a different unit (partial pressure) than all other species involved (molar concentration). If the concentrations of both nitrite and nitric oxide are expressed in mol l^{-1}, then the E_M (pH 7) = 189 mV versus NHE for the equilibrium $NO_2^- + 2H^+ + e^- \rightleftarrows NO_{(aq)} + H_2O$ (chapter 3). An interesting, and unexpected, result was that under physiological conditions (slightly alkaline pH and in the presence of physiological electron donors) the equilibrium strongly favours the substrates rather than the products (chapter 3).